Misan Journal of Engineering Sciences ISSN: 2957-4250
Vol. 4, No. 1, June 2025 ISSN-E: 2957-4242

Analysis of the Mechanical Behaviour of a Tube Confined within a Granular Medium

Sajid K. ZEMAM[1,*], Mohamad JRAD[2], Norman MATHIEU[2], Mahdia HATTAB[2]

[1] Civil Engineering Department/ Engineering College/Misan University /Misan, Iraq
[2] Université de Lorraine, CNRS, Arts et Métiers ParisTech, LEM3, F-57000 Metz, France

**Corresponding author E-mail: sajid.kamil@uomisan.edu.iq*

(Received 22 May, Revised 20 June, Accepted 21 June)

Abstract: Understanding the mechanical behaviour of confined cylindrical shells is essential for the long-term stability of geotechnical structures such as buried pipelines and well casings. These structures often experience lateral loading when embedded in granular materials or rock, resulting in complex solid-to-solid interactions. This study investigates the stability of a metallic tube confined within such media through a combination of experimental and numerical approaches. A laboratory-scale test setup was developed to conduct controlled experiments on instrumented metallic tubes. The setup enabled the determination of the critical buckling pressure, identification of post-buckling stability loss, and monitoring of local deformations leading to failure. The study revealed that both nature (homogeneous vs. bi-material) and the stiffness of the confining medium significantly influence the critical buckling pressure and the angular extension of the single-lobe deformation pattern. Complementary finite element simulations were performed to interpret the experimental findings. The numerical results showed excellent agreement with the experimental data, validating the modelling approach. Simulations further provided detailed insights into the initiation and evolution of buckling prior to structural instability under increasing lateral confinement. These findings contribute to a deeper understanding of confined shell behaviour and have practical implications for the design and assessment of underground tubular structures.

Keywords: Single lobe Buckling, Confined Cylindrical Shells, Critical Pressure, Numerical Simulation, Finite Element Modelling, Lateral Loading

1. Introduction

Thin-walled cylindrical shells subjected to external confinement are widely utilised in geotechnical and civil infrastructure systems, particularly in underground applications. These structural elements serve critical functions in a variety of engineering domains: as well casings in oil and gas wells, where they act as the primary mechanical barrier preserving borehole integrity [1,2]; as sleeved piles designed to improve the seismic resilience of deep foundations [3]; and as buried pipelines that are laterally confined by backfilled soils [4]. Owing to their geometric slenderness and material efficiency, these shells are susceptible to buckling under compressive or lateral loads, a failure mode that can significantly compromise their structural performance and serviceability.

Buckling, a classical form of elastic instability, is characterised by a sudden and disproportionate lateral deformation triggered by axial or external pressure, often leading to abrupt loss of load-carrying capacity. This phenomenon is particularly critical in thin-walled structures exposed to varying confinement conditions, whether rigid, semi-rigid, or discontinuous. Foundational work by Bresse [5] and Bryan [6] established the fundamental criteria governing the elastic buckling of unconfined cylindrical shells.

DOI: https://doi.org/10.61263/mjes.v4i1.153

However, the presence of a surrounding medium—such as compacted soil, grout, or cementitious materials—substantially alters the deformation mechanics and energy dissipation characteristics of the system. External confinement limits radial outward deformation and, counterintuitively, can encourage the formation of localised inward buckling modes with reduced wavelengths.

The influence of confinement on shell stability has been extensively investigated through analytical formulations, numerical simulations, and experimental campaigns. Seminal studies by Glock [7], Cheney [8], and El-Sawy [9] introduced predictive models for estimating the critical buckling pressure of cylindrical shells under confinement. These models incorporate geometric nonlinearities such as initial ovality, geometric imperfections, and interface irregularities. Findings from these investigations indicate that confinement can either enhance or reduce buckling resistance, depending on the stiffness and continuity of the surrounding medium. More recent full-scale experimental investigations by Kyriakides and Lee [10], and Wang and Koizumi [11], further revealed the complexity of post-buckling behaviour in confined systems, particularly when non-ideal contact conditions or material discontinuities exist at the interface between the shell and the filler medium.

Within this context, the role of the cementitious interface—defined as the mechanical interface between the steel shell and the encasing grout—becomes of central importance in evaluating the system's overall stability. This interface governs the transfer of stresses, the initiation of buckling, and the distribution of contact pressure along the structure–soil boundary. Its stiffness, bonding integrity, and continuity directly influence the deformation patterns and the energy dissipation capacity of the composite system. Experimental findings by Webb, Trebicki, and Smulders [12] have demonstrated that cement grout, when placed beneath or around buried conduits, significantly mitigates vertical and lateral displacements and reduces stress concentration zones, thereby delaying the onset of structural instability. This form of partial confinement effectively acts as a localised rigid support, increasing the system's confinement stiffness and enhancing its buckling resistance.

The critical effect of confinement stiffness was further quantified by Nguyen [13] in his doctoral investigations on steel shells subjected to lateral pressure under different backfill conditions. His experiments reported substantial improvements in buckling capacity—up to 360% for dry sand and 400% for saturated sand—when compared to unconfined cases. The buckling mode observed was consistently a single inward-propagating lobe, with a decreasing wavelength correlated to increasing stiffness of the surrounding material. These observations emphasise the dominant role played by confinement stiffness in dictating both the critical pressure and deformation morphology of the shell.

Despite these advances, several research gaps remain. In particular, the combined effects of imperfect bonding, interface stiffness, and complex loading paths on the buckling behaviour of confined shells are not yet fully understood. Existing models often oversimplify the interface conditions or neglect post-buckling responses under real-world loading scenarios.

The present research aims to fill this gap by systematically investigating the structural behaviour of thin-walled steel cylinders subjected to external pressure in the presence of a cementitious confining layer. The study focuses on characterising the influence of interface stiffness, bonding quality, and material discontinuities on buckling initiation and post-buckling response. In doing so, this work seeks to contribute a more comprehensive understanding of the instability mechanisms governing confined shell systems, ultimately enabling the development of robust, reliability-based design methodologies for buried and confined tubular structures in civil and geotechnical engineering.

2. Confined Buckling Test

This experimental study investigates the key aspects of buckling in confined steel cylinders in order to deepen our understanding of this phenomenon. Buckling, defined as a structural failure due to instability, has been the subject of previous experimental research aimed at identifying its mechanisms and implications, particularly in the case of steel cylinders. However, the influence of the confining medium has not been experimentally investigated.

2.1. Steel Specimens

The specimens consist of API 5L X65 steel tubes. The mechanical properties of the steel were determined in the laboratory through uniaxial tensile tests conducted on samples extracted from the same steel tube used to prepare the buckling test specimens. The results are shown in Table 1 below.

Table 1: Mechanical Properties of API 5L X65 Steel under Uniaxial Loading

Material	Young's Modulus E (MPa)	Poisson's Ratio	Yield Strength σ_y (MPa)
API 5L X65	205000	0.3	446

In the tests, the cylindrical specimen has a height of 480 mm, a mean radius of 80 mm, and a wall thickness of 2 mm (yielding an R/t ratio of 40). Steel rings are positioned at both ends of the shell (Figure 1) to ensure controlled and reproducible boundary conditions. In this case, the configuration corresponds to clamped boundary conditions. To secure the connection between the shell and the rings, a low-melting-point metal is used.

Fig. 1 (a) Cylindrical shell, (b) Upper and lower steel rings

2.2 Confining Medium

S28 sand is used as the confining medium. In our tests, a type of HN 31 sand (Hostun RF S28), supplied by the company Sibelco, was employed for this purpose. This granular material consists of quartz-based silica sand with a medium to coarse grain size, and is dried, with a particle size distribution ranging from 0.2 mm to 0.5 mm (Figure 2). Its internal friction angle is 32º.

To evaluate its behaviour, a confined compression test was conducted using a Zwick testing machine with a capacity of 100 kN. The sample tested was a cylinder with a diameter of 70 mm and a height of 150 mm. The applied axial force reached 70 kN, corresponding to a vertical stress of 18.2 MPa, under which a vertical strain of 7.5% was observed.

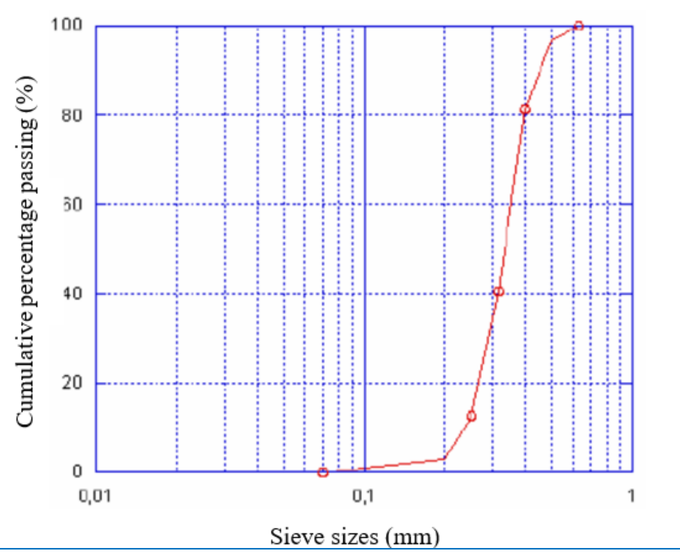

Fig. 2 Particle Size Distribution Curve of Sand Sample S28

2.3. Instrumentation

To accurately describe the hoop strains on the cylinder wall, a set of nine to fourteen strain gauges (intended to provide more detailed information and a more precise representation of the cylinder's instability) was installed at mid-height (h/2) of the cylindrical shell. This configuration enables a more refined depiction of the structure's unstable behaviour. The sensors used are KYOWA KFGS-5-120-C1-11 strain gauges, with a gauge length of 9.4 mm and a width of 2.8 mm, capable of measuring strains up to 5%. These gauges were arranged in a regular angular configuration, with intervals of 40° between each pair. To ensure protection against moisture and external agents, the gauges were coated with a thin layer of epoxy. Figure 3 illustrates the adopted instrumentation layout.

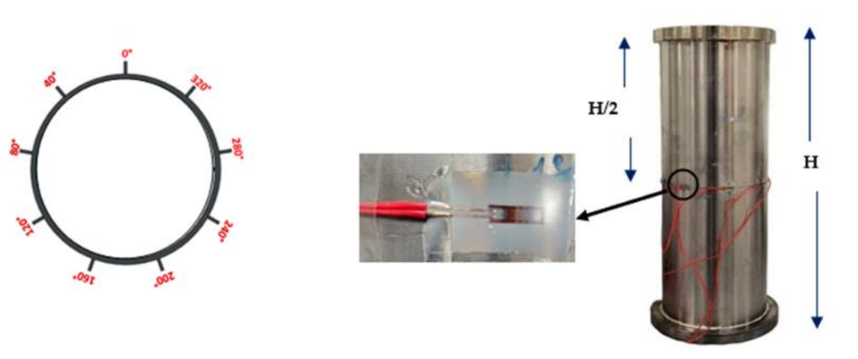

Fig. 3 Instrumentation diagram of a clamped cylindrical specimen

2.4. Testing Setup and Experimental Protocol

To study the behaviour of a confined thin shell under radial loading, an experimental setup was developed at INSA Lyon [13] and subsequently improved at LEM3 (Figure 4). The radial load is applied to the confining medium via an inflatable bladder filled with pressurised oil, connected to an electric pump and equipped with a pressure sensor at its inlet.

Since the bladder undergoes minimal deformation, the internal pressure within the bladder is considered equivalent to that applied to the filling material. However, this pressure does not directly represent the stress exerted on the shell. To prevent any axial displacement of the specimen, the entire assembly is placed under a 1200 kN Zwick press, allowing precise control of position (imposed displacement) and measurement of axial load. A preload of 2.5 kN is applied to ensure initial contact between the press and the specimen. Data acquisition is performed at a sampling frequency of 5 Hz using a data acquisition unit connected to a PC.

The instrumented specimen is installed at the center of the setup, after which the space between the shell and the inflatable bladder is filled with Hostun S28 sand. A metallic cover is then placed to hold the material in position. The test begins by bringing the press crosshead into contact with the cover, followed by the application of the preload.

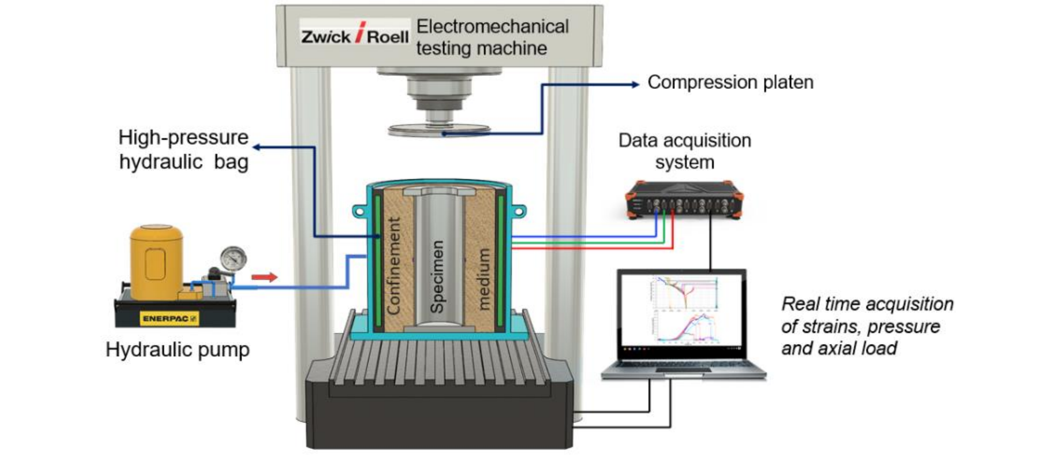

Fig. 4 Experimental device

3. Numerical Modelling

The numerical model employed in this study comprises a steel cylinder confined by a sand layer, with boundary conditions replicating the experimental setup. The commercial software Abaqus is used. The actual geometry of the shell (obtained via 3D scanning) was imported into the model. The shell is simulated using S4R elements (four-node shell elements) with a mesh size of 8 mm. It is clamped at both ends.

The confinement is modelled as a hollow cylinder of the same height, with an inner radius of 81 mm and an outer radius of 170 mm, resulting in a thickness of 89 mm. This domain is simulated with C3D20R elements (20-node quadratic solid elements) using a mesh size of 12 mm.

A surface-to-surface contact interaction is defined between the shell and the confining medium. The contact properties include normal non-penetration and tangential friction.

Figure 5 illustrates the system: the shell and the sand. The ends are fully constrained in translation and rotation.

The lateral loading is applied through radial displacement of the outer nodes of the confining medium. Radial reactions are then extracted to calculate the average pressure on the outer lateral surface of the sand by dividing the total force by the external lateral area.

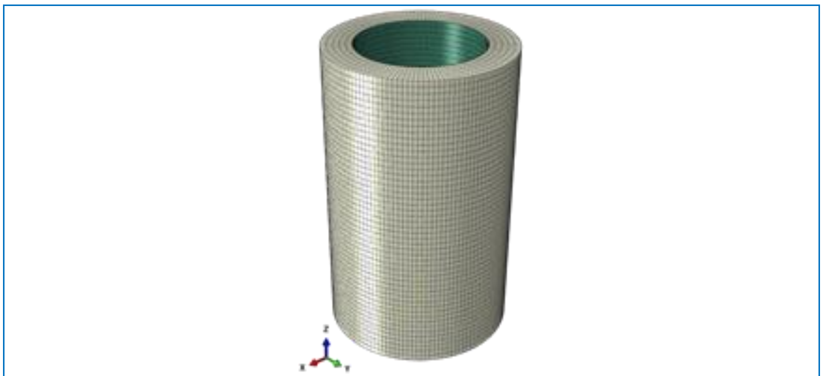

Fig. 5 Assembly in Abaqus of the cylindrical shell (in green) and the confining medium (in grey).

4. Results

At the end of the numerical simulation, it was observed that the cylinder had lost its stability, revealing a single-phase buckling after exceeding the critical load. Buckling occurred along the entire length of the cylinder and was identified as inward (closed type) buckling. When comparing these results with experimental observations, it was found that the buckling shape was similar to that obtained in the numerical simulation (Figure 6).

The numerical results show that the external pressure applied to the confined medium (sand) gradually increases over time, reaching a maximum value of 18.7 MPa at t = 190.275 seconds. Thereafter, the pressure begins to gradually decrease to 18.2 MPa—representing a 2.5% reduction from the peak pressure over a duration of 9.7 seconds. This decrease is attributed to the buckling of the cylinder. These results are consistent with experimental observations, in which the maximum recorded pressure was 18.25 MPa before a progressive decrease of 3.5% over a period of 2 seconds (Figure 7).

It is observed from Figure 7 that the drop in external pressure at the moment of buckling occurs more rapidly in the numerical simulation than in the experimental tests. This difference can primarily be attributed to several modelling-related factors in the numerical simulation.

First, the implicit dynamic analysis used in Abaqus generally does not account for viscoelastic effects or time-dependent phenomena such as creep and energy dissipation, which can slow down the real system's response. Second, the loading conditions in the simulation—often applied as a radial displacement at a constant speed—may be faster than those in the real experiment, resulting in an accelerated model response. Furthermore, the complex interaction between the cylinder, the grout, and the loading medium (such as a hydraulic cushion) is often simplified in the numerical model, neglecting damping, compressibility, or flow resistance effects that may be present in the experimental setup. Finally, the nonlinear mechanical properties of the grout (such as progressive cracking, damage, and post-peak behaviour) are often difficult to represent accurately, which directly influences the buckling progression.

These simplifications thus lead to a faster prediction of stability loss in the numerical simulation, highlighting the need for fine calibration of model parameters to improve the correlation with experimental results.

For the calculation of cylinder strains in the numerical simulation, it was assumed that the buckling location was identical to that observed in the experimental test (at 270°). The strains were then extracted at positions approximately corresponding to those of the strain gauges used in the experiments, and a comparison between numerical and experimental results was carried out (Figure 8).

The analysis of the results highlights a notable similarity between the strain behaviour obtained numerically and that observed experimentally. The pressure–strain curve initially shows a linear phase, characteristic of homogeneous and negative elastic deformations. This phase is followed by a gradual divergence of the curves, indicating increasing material heterogeneity, along with oscillations marking the transition to plastic behaviour.

In the numerical simulations, this departure from linearity is observed at a pressure of 10 MPa, whereas in the experimental tests it occurs at (8-9) MPa. In both cases, the end of the elastic zone corresponds to a strain of approximately 0.3%, marking the transition from elastic to plastic behaviour.

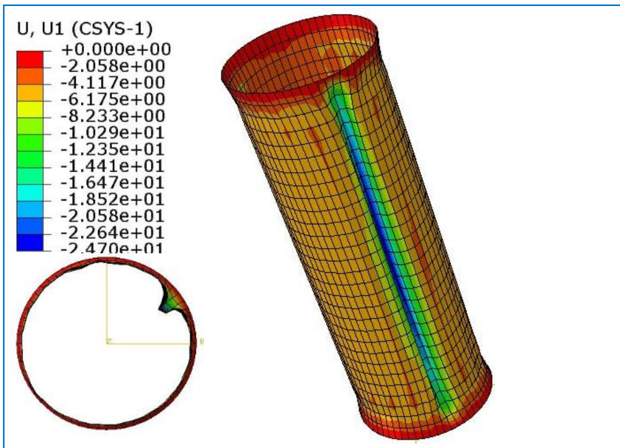

A: Numerical Results

B: Experimental Results

Fig 6: Final buckling shape for the numerical simulation and the experimental test.

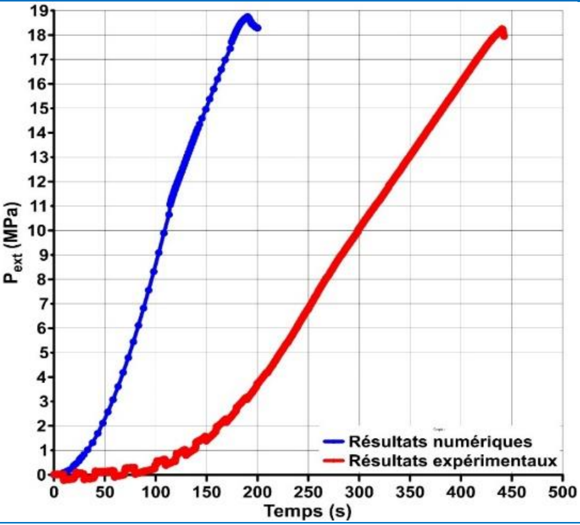

Fig 7: Evaluation of pressure as a function of time for the numerical simulation and the experimental test.

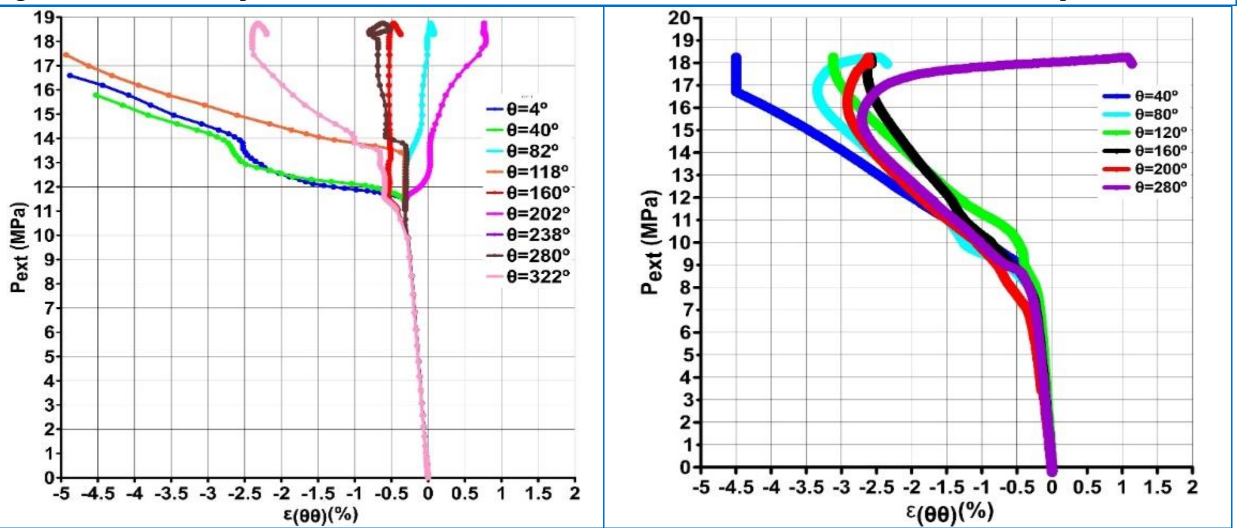

A: Numerical Results	B: Experimental Results

Fig 8: Pressure as a function of deformation for the numerical simulation and experimental test.

5. Conclusion

This study has enhanced the understanding of the mechanical behaviour of steel cylindrical shells subjected to confinement by a granular material, specifically S28 sand.

Through a rigorous experimental approach complemented by advanced numerical modelling, it was possible to accurately characterise the buckling mechanism under confinement.

The experimental results highlighted a single-lobe buckling mode affecting the entire shell, occurring after the critical pressure was exceeded. The strong agreement between experimental observations and numerical predictions validates the relevance of the model used, both in terms of the buckling mode and the critical values of pressure and strain.

The finite element modelling proved particularly effective in capturing complex nonlinear phenomena such as large displacements, material plasticity, and contact interaction with the confining medium. The numerical approach not only faithfully reproduced the experimental results but also provided additional insight into the initiation and progressive development of buckling.

Author Contributions: The authors contributed to all parts of the current study.

Funding: This study received no external funding.

Conflicts of Interest: The authors declare no conflict of interest.

References

[1] A. I. Mohammed, B. Oyeneyin, B. Atchison, and J. Njuguna (2019), “Casing structural integrity and failure modes in a range of well types: A review”, J. Nat. Gas Sci. Eng., 68(–), 102898. https://doi.org/10.1016/j.jngse.2019.05.011
[2] P. Sun, T. Luo, B. Wang, and W. Yang (2022), “Sinusoidal buckling behaviour of surface casing with negative friction in thawing permafrost”, J. Petrol. Sci. Eng., 208(–), 109616. https://doi.org/10.1016/j.petrol.2021.109616
[3] S. Thusoo, S. Kono, J. Hamada, and Y. Asai (2020), “Performance of precast hollow steel-encased high-strength concrete piles”, Engineering Structures, 204(–), 109995. https://doi.org/10.1016/j.engstruct.2019.109995
[4] I. D. Moore and E. T. Selig (1990), “Use of continuum buckling theory for evaluation of buried plastic pipe stability”, ASTM Special Technical Publication, 1093, 344–359.
[5] J. A. C. Bresse (1866), Cours de mécanique appliquée (2nd ed.), Paris, France.
[6] G. H. Bryan (1888), “Application of the energy test to the collapse of a long thin pipe under external pressure”, Cambridge Philosophical Society Proceedings, 6, 287–292.
[7] D. Glock (1977), “Überkritisches Verhalten eines starr ummantelten Kreisrohres bei Wasserdrunck von aussen und Temperaturdehnung (Post-critical behavior of a rigidly encased circular pipe subject to external water pressure and thermal extension)”, Der Stahlbau, 7, 212–217.
[8] J. A. Cheney (1971), “Pressure buckling of ring encased in cavity”, Journal of Engineering Mechanics, 97(2), 333–342.
[9] K. El-Sawy and I. D. Moore (1998), “Stability of loosely fitted liners used to rehabilitate rigid pipes”, Journal of Structural Engineering, ASCE, 124(11), 1350–1357.
[10] S. Kyriakides and L.-H. Lee (2005), “Buckle propagation in confined steel tubes”, International Journal of Mechanical Sciences, 47(4), 603–620. https://doi.org/10.1016/j.ijmecsci.2004.11.009
[11] J. H. Wang and A. Koizumi (2017), “Experimental investigation of buckling collapse of encased liners subjected to external water pressure”, Engineering Structures, 151, 44–56. https://doi.org/10.1016/j.engstruct.2017.08.008
[12] M. C. Webb, D. D. P. Trebicki, and P. A. Smulders (2002), “Field testing and buckling strength of buried large-diameter thin-walled steel pipes”, Proceedings of the ASCE Pipeline Division Specialty Conference. https://doi.org/10.1061/40641(2002)69
[13] T. Nguyen (2017), Flambage sous contact d’une coque cylindrique soumise à pression externe, Doctoral dissertation, Université de Lyon.
[14] D. Vasilikis and S. A. Karamanos (2011), “Buckling design of confined steel cylinders under external pressure”, J. Pressure Vessel Technol., 133(1), 1–9.